Jia-Ming Li*, Kun-Huan He, Zhong-Feng Shi, Hui-Yuan Gao and Yi-Min Jiang*

Syntheses and crystal structures of two new silver–organic frameworks based on *N*-pyrazinesulfonyl-glycine: weak Ag···O/N interaction affecting the coordination geometry

DOI 10.1515/znb-2016-0134
Received May 25, 2016; accepted June 22, 2016

Abstract: Two new metal–organic frameworks, namely, $[Ag_2(L)]_n$ (**1**) and $\{[Ag_{2.5}(L)(bpy)_2]\cdot(NO_3)_{0.5}\cdot(H_2O)_{4.5}\}_n$ (**2**), where H_2L = *N*-pyrazinesulfonyl-glycine and bpy = 4,4′-bipyridine, have been synthesized and characterized by single-crystal X-ray diffraction, IR spectroscopy, and elemental analysis. X-ray diffraction crystallographic analyses indicate that **1** displays a silver carboxylate-sulfonamide layer structure containing an uncommon heptanuclear $[Ag_7]$ cluster wherein four silver(I) atoms form an Ag_4 plane with in a three-connected (6, 3) net. The molecular structure of **2** has three crystallographically independent two-coordinate Ag centers with an intersecting Ag-bpy chain structure in a six-connected (3, 6) or a four-connected (4, 4) topology. The L^{2-} ligand serves as a μ_7-(η_2-O,N), (η_2-O′,N′), O,O″,O‴,N,N″ ligand in **1** and as a μ_3-(η_2-O,N), N,O′ ligand in **2**. In the crystal, a 3D supramolecular architecture is formed by coordinative bonding in **1**, but through O–H···O bonding as well as π···π stacking in **2**. The two compounds show a combination of coordinative bonds, ligand-supported Ag···Ag interactions and weak Ag···O/N coordinative interactions in the solid state.

***Corresponding authors: Jia-Ming Li,** Guangxi Colleges and Universities Key Laboratory of Beibu Gulf Oil and Natural Gas Resource Effective Utilization, College of Petroleum and Chemical Engineering, Qinzhou University, Qinzhou 535011, P.R. China, e-mail: ljmmarise@163.com; and **Yi-Min Jiang,** School of Chemistry and Pharmacy, Guangxi Normal University, Key Laboratory for the Chemistry and Molecular Engineering of Medicinal Resources (Ministry of Education), Guilin 541004, P.R. China, e-mail: ymjiang@mailbox.gxnu.edu.cn
Kun-Huan He and Zhong-Feng Shi: Guangxi Colleges and Universities Key Laboratory of Beibu Gulf Oil and Natural Gas Resource Effective Utilization, College of Petroleum and Chemical Engineering, Qinzhou University, Qinzhou 535011, P.R. China
Hui-Yuan Gao: School of Chemistry and Pharmacy, Guangxi Normal University, Key Laboratory for the Chemistry and Molecular Engineering of Medicinal Resources (Ministry of Education), Guilin 541004, P.R. China

Keywords: 4,4′-bipyridine; crystal structure; metal–organic frameworks; *N*-pyrazinesulfonyl-glycine; silver(I) complex.

1 Introduction

Silver–organic frameworks as an important class of crystalline materials have been attracting considerable attention due to their extensive applications in luminescence, gas adsorption, magnetic switching devices, catalysis, and so on [1–5]. Ag metal–organic frameworks (MOFs) not only show more structural diversity, but also exhibit synergistic effects between organic and inorganic components compared with other MOFs. The assemblies of these MOFs are heavily influenced by many factors such as the pH value, the molar ratio of the molecular components, solvent, steric requirement of the counterions, and reaction temperature, together with the coordination nature of metal ions and organic ligands [6–10]. MOFs derived from the "softer" Ag^+ ions demonstrate a unique behavior in comparison to other transition metals [11–15]. As is well known, the Ag(I) ion commonly has a coordination number varying from 2 to 4 and is accompanied by a variety of coordination geometries such as linear, trigonal, and tetrahedral, which give rise to novel coordination networks [16–19]. An interesting aspect of the silver(I) complexes is the common observation of short Ag···Ag contacts (termed argentophilicity, Ag(I)···Ag(I) < 3.4 Å), which have been proved to be one of the most important factors contributing to the formation of such complexes and their special properties [20]. In recent years, the studies of Ag-MOFs based on functional organic polycarboxylate ligands have made great progress [21–25]. However, the rational design and synthesis of Ag-MOFs with unique structure and function is a very intricate process, and still remains a big challenge.

In our continuous efforts to study the coordination chemistry of *N*-pyrazinesulfonyl-glycine (H_2L) ligand with

its versatile functional groups, we have shown that H_2L can also be self-assembled with the coordinatively flexible silver(I) cation. We report here two novel silver(I) polymers, $[Ag_2(L)]_n$ (**1**) and $\{[Ag_{2.5}(L)(4,4'\text{-bipy})_2]\cdot(NO_3)_{0.5}\cdot(H_2O)_{4.5}\}_n$ (**2**), with regard to syntheses, crystal structures, and IR spectra. Compound **1** is a 3D supramolecular framework having a silver(I)-carboxylate-sulfonamide layer constructed from heptanuclear $[Ag_7]$ clusters and L^{2-} ligands, whereas **2** is a 2D supramolecular network formed by silver(I)-bpy intersecting chains and L^{2-} ligands through coordinative bonds, ligand-supported Ag···Ag interactions, and weak Ag···O/N coordinative interactions (Scheme 1).

2 Results and discussion

2.1 Description of the crystal and molecular structure of $[Ag_2(L)]_n$ (1)

The single-crystal X-ray diffraction structural analysis has revealed that **1** is a 3D coordination polymer, whose asymmetric unit comprises two crystallographically nonequivalent Ag(I) cations and a doubly deprotonated chelating L^{2-} ligand. As is shown in Fig. 1a, two unique Ag(I) ions display two types of coordination modes (neglecting the weak Ag···O and Ag···Ag interactions).

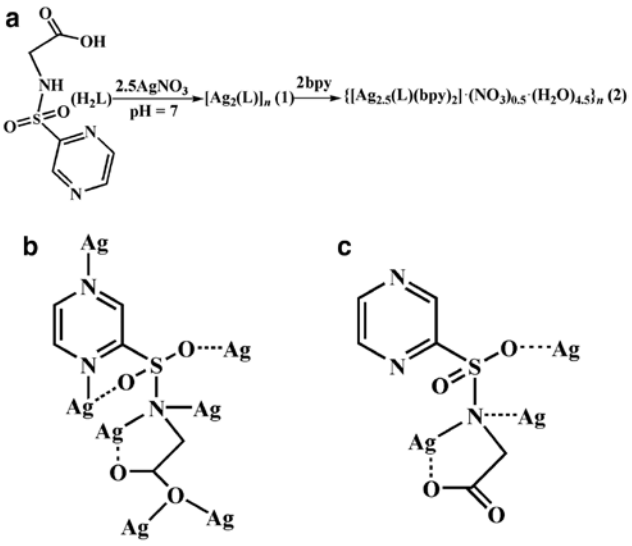

Scheme 1: (a) The synthesis for **1** and **2**; (b) view of the coordination mode of the L^{2-} ligand in **1**; (c) view of the coordination mode of the L^{2-} ligand in **2**.

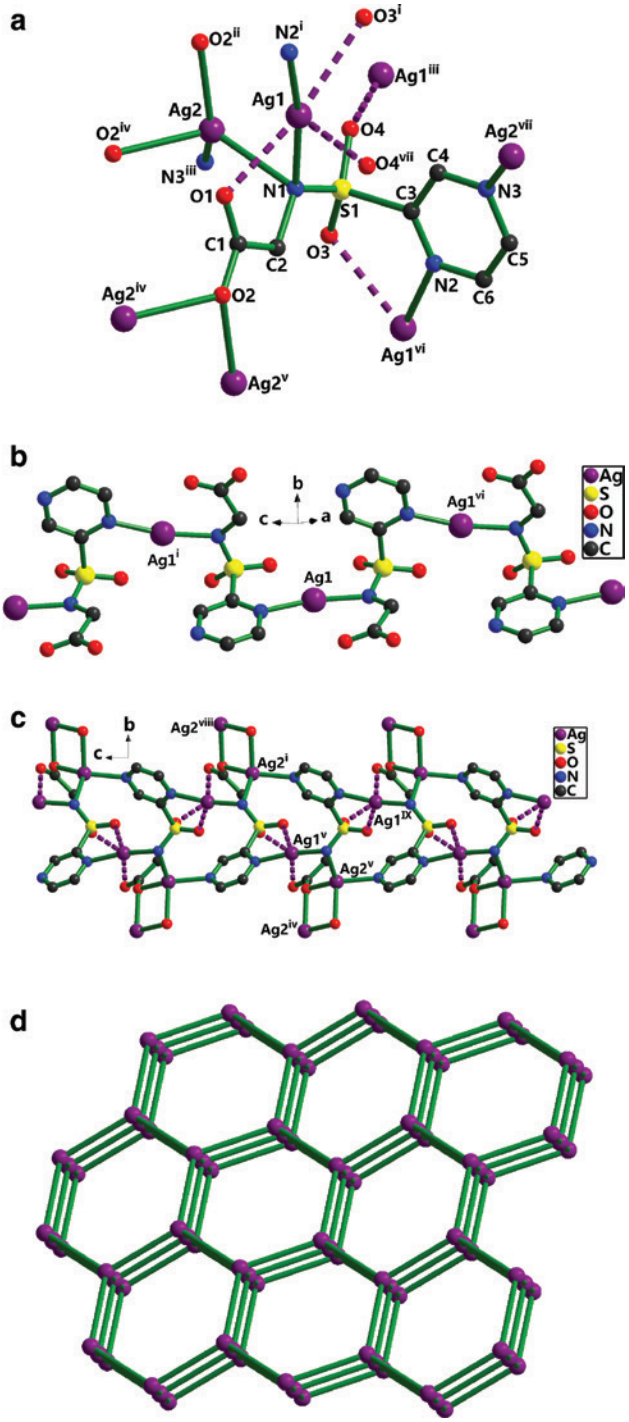

Fig. 1: (a) The coordination environment for Ag^+ in **1** (symmetry codes: i: $x-1/2, -y+1/2, z+1/2$; ii: $x-1, y, z$; iii: $x-1/2, -y+1/2, z-1/2$; iv: $-x+2, -y, -z$; v: $x+1, y, z$; vi: $x+1/2, -y+1/2, z-1/2$; vii: $x+1/2, -y+1/2, z+1/2$). (b) The 1D coordination framework of Ag1 in **1**. (c) View of the 3D coordination grid framework along the *a* axis (symmetry codes: i: $x-1/2, -y+1/2, z+1/2$; iv: $-x+2, -y, -z$; v: $x+1, y, z$; viii: $-x+5/2, y+1/2, -z+1/2$; ix: $x+3/2, -y+1/2, z-1/2$). (d) The simplified topology (6, 3) considering the Ag_7 cluster as a node and the linkers representing L^{2-}.

Ag1 is coordinated by two nitrogen atoms (Ag1–N1 = 2.222(5) Å, Ag1–N2^{i} = 2.249(5) Å, symmetry code: i: $x-1/2$, $-y+1/2$, $z+1/2$) from two different L^{2-} anions with an N1–Ag1–N2^{i} bond angle of 168.67(19)°, whereas Ag2 is ligated by two oxygen donors (Ag2–O2^{ii} = 2.310(5) Å, Ag2–O2^{iv} = 2.363(4) Å) and two nitrogen atoms (Ag2–N1 = 2.399(5) Å, Ag2–N3^{iii} = 2.327(6) Å) (symmetry codes: ii: $x-1$, y, z; iii: $x-1/2$, $-y+1/2$, $z-1/2$; iv: $-x+2$, $-y$, $-z$) from four discrete L^{2-} ligands (Table 1). Ag2 adopts distorted tetrahedral coordination geometry with the bond angles spanning the range from 87.08(16)° to 137.9(2)°, with $\tau_4 = 0.4$ for Ag2. The distortion of the tetrahedron can be indicated by the calculated value of the τ_4 parameter introduced by Houser [26] to describe the geometry of a four-coordinated transition metal system (for perfect tetrahedral geometry, $\tau_4 = 1$). The Ag–O/N bond lengths are comparable to those observed in related silver(I) compounds [22–25]. However, the distances Ag1–O1 (2.570(5) Å), Ag1–O3^{i} (2.660(7) Å), and Ag1–O4^{vii} (2.741(5) Å) (symmetry code: vii: $x+1/2$, $-y+1/2$, $z+1/2$) are beyond the range of 2.32–2.52 Å for silver(I) carboxylates but still shorter than the sum of van der Waals radii (3.24 Å) of the Ag and oxygen atoms, suggesting the existence of significant Ag···O interactions and explaining the deviation of the Ag(I) center from perfect linear-shaped geometry. Within this unit, the Ag1···Ag2 distance is 2.964(8) Å, implying the existence of ligand-supported argentophilic interactions. Taking weak Ag–O interactions into account, the coordination mode of L^{2-} can be described as μ_7-(η_2-O,N), (η_2-O′,N′), O,O″,O‴,N,N″ in **1**, which has never been reported in Ag-containing compounds. A better insight into the nature of this intricate heptanuclear silver cluster can be achieved by removing the organic L^{2-} ligand. Four Ag ions (Ag1^{iii}/Ag1^{vi}/Ag2/Ag2^{v}) are co-planar and form an Ag_4 plane with the Ag1^{iii}/Ag2 = Ag1^{vi}/Ag2^{v} and Ag1^{iii}/Ag1^{vi} = Ag2/Ag2^{v} (for symmetry codes see Fig. 1a) separations of 5.19(7) and 5.92(1) Å, respectively. The adjacent Ag1 ions are connected by one L^{2-} to give an [Ag(L)] covalent chain along the *c* axis (Fig. 1b), which is further extended by the bonds Ag2–N1 and Ag2–N3 leading to a layer. As shown in Fig. 1c, an overall 3D supramolecular framework results from the linkage of neighboring layers through Ag2–O2 bonds. From the topological point of view, each Ag_7 cluster links three L^{2-} units as a three-connected node, and each L^{2-} ligand bridges two Ag_7 clusters acting as a linker. The 3D MOF topology of **1** can be classified as a three-connected (6, 3) net (Fig. 1d). There are no remarkable hydrogen bonds or π stacking interactions in **1**, but a weak nonclassical C–H···O contact (Table 2).

Table 1: Selected bond lengths (Å) and angles (deg) for **1** and **2** with estimated standard deviations in parentheses.

Compound **1**[a]			
Ag1–N1	2.222(5)	Ag1–N2^{i}	2.249(5)
Ag1–O1	2.570(5)	Ag1–Ag2	2.9636(8)
Ag2–O2^{ii}	2.310(5)	Ag2–N3^{iii}	2.327(6)
Ag2–O2^{iv}	2.363(4)	Ag2–N1	2.399(5)
N1–Ag1–N2^{i}	168.67(19)	N1–Ag1–O1	70.13(17)
Ag1–N1–Ag2	79.68(17)	N1–Ag1–Ag2	52.79(13)
N2^{i}–Ag1–O1	98.54(18)	O1–Ag1–Ag2	72.99(15)
N2^{i}–Ag1–Ag2	125.20(14)	O2^{ii}–Ag2–N3^{iii}	137.9(2)
O2^{ii}–Ag2–O2^{iv}	87.08(16)	O2^{ii}–Ag2–N1	113.79(18)
N3^{iii}–Ag2–O2^{iv}	96.99(18)	O2^{iv}–Ag2–N1	122.70(17)
N3^{iii}–Ag2–N1	99.10(19)	N3^{iii}–Ag2–Ag1	141.20(14)
O2^{ii}–Ag2–Ag1	66.38(13)	N1–Ag2–Ag1	47.53(13)
O2^{iv}–Ag2–Ag1	116.92(12)	Ag2^{v}–O2–Ag2^{iv}	92.92(16)
Compound **2**[b]			
Ag1–N4	2.224(4)	Ag1–N1	2.281(4)
Ag1–O1	2.566(5)	Ag1–N1^{i}	2.626(4)
Ag1–Ag1^{i}	2.8777(9)	Ag2–N6	2.164(4)
Ag2–N5	2.170(4)	Ag3–N7	2.147(4)
S1–O3	1.437(4)		
N4–Ag1–N1	154.35(16)	O1–Ag1–N1^{i}	143.72(16)
N4–Ag1–O1	98.14(16)	N4–Ag1–Ag1^{i}	141.01(12)
N1–Ag1–O1	70.99(14)	N1–Ag1–Ag1^{i}	59.88(10)
N4–Ag1–N1^{i}	93.94(15)	O1–Ag1–Ag1^{i}	118.52(11)
N1–Ag1–N1^{i}	108.59(12)	N1^{i}–Ag1–Ag1^{i}	48.71(9)
N6–Ag2–N5	177.53(18)	N7–Ag3–N7^{ii}	180

[a]Symmetry codes: i: $x-1/2$, $-y+1/2$, $z+1/2$; ii: $x-1$, y, z; iii: $x-1/2$, $-y+1/2$, $z-1/2$; iv: $-x+2$, $-y$, $-z$; v: $x+1$, y, z.
[b]Symmetry code: i: $-x+1$, $-y$, $-z+1$; ii: $-x+2$, $-y+4$, $-z+2$.

2.2 Description of the crystal and molecular structure of {[$Ag_{2.5}$(L)(4,4′-bipy)$_2$]·(NO_3)$_{0.5}$·(H_2O)$_{4.5}$}$_n$ (2)

Single-crystal X-ray diffraction analysis has revealed that **2** crystallizes in the triclinic space group $P\bar{1}$ as a 2D supramolecular network generated from a combination of coordinative bonds, ligand-supported Ag···Ag interactions, and weak Ag···O/N coordinative interactions. The asymmetric unit of **2** consists of two and a half crystallographically unique Ag(I) ions, one L^{2-} dianion, a half of an NO_3^- ion, two 4,4′-bipy ligands, as well as four and a half solvent water molecules. As shown in Fig. 2a, the Ag1 and Ag2 atoms (neglecting the weak Ag···O, Ag···N, and Ag···Ag interactions) adopt a distorted linear geometry with two nitrogen atoms from one L^{2-} and one bpy for Ag1, and two different bpy for Ag2, whereas Ag3 is located at a center of symmetry, connecting two symmetry-related bpy with a bond N7–Ag3–N7^{ii} angle of 180° (symmetry code: ii: $-x+2$, $-y+4$, $-z+2$). The preferred coordination of the

Table 2: Hydrogen bond geometry (Å, deg) in crystalline **1** and **2** with estimated standard deviations in parentheses.

D–H···A	d(D–H)	d(H···A)	d(D···A)	∠(DHA)
Compound **1**[a]				
C5–H5···O1^{viii}	0.93	2.51	3.407(9)	163
Compound **2**[b]				
O8–H8B···O7^{iii}	0.85	2.49	3.26(2)	150
O9–H9A···O10^{iv}	0.85(6)	1.97(7)	2.685(9)	141(10)
O9–H9B···O5	0.85(7)	2.04(10)	2.744(11)	139(8)
O10–H10A···O11^{v}	0.84(7)	2.18(9)	2.761(9)	125(8)
O10–H10B···O1^{iv}	0.84(7)	2.00(8)	2.808(8)	162(8)
O11–H11A···O2^{vi}	0.85(6)	1.89(6)	2.737(9)	173(19)
O11–H11B···O5	0.85(7)	2.13(7)	2.832(10)	140(7)
O11–H11B···O7	0.85(8)	2.48(8)	3.204(18)	144(7)
O12–H12B···O2^{vi}	0.85(6)	2.16(10)	2.911(11)	147(11)
C4–H4···O4	0.93	2.55	2.911(8)	104
C6–H6···O6	0.93	2.60	3.405(13)	146
C8–H8···O9	0.93	2.50	3.286(9)	142
C10–H10···O6^{iv}	0.93	2.51	3.407(15)	162
C12–H12···O3^{iv}	0.93	2.46	3.187(7)	135
C12–H12···N2^{iv}	0.93	2.62	3.424(8)	146
C16–H16···O12	0.93	2.52	3.341(9)	148
C25–H25···O9^{vii}	0.93	2.57	3.375(9)	144

[a]Symmetry codes: viii: $-x+5/2$, $y+1/2$, $-z+1/2$.
[b]Symmetry codes: iii: $x+1$, y, z; iv: $-x+1$, $-y+1$, $-z+1$; v: x, y, $z-1$; vi: x, $y+1$, z; vii: $-x+1$, $-y+2$, $-z+2$.

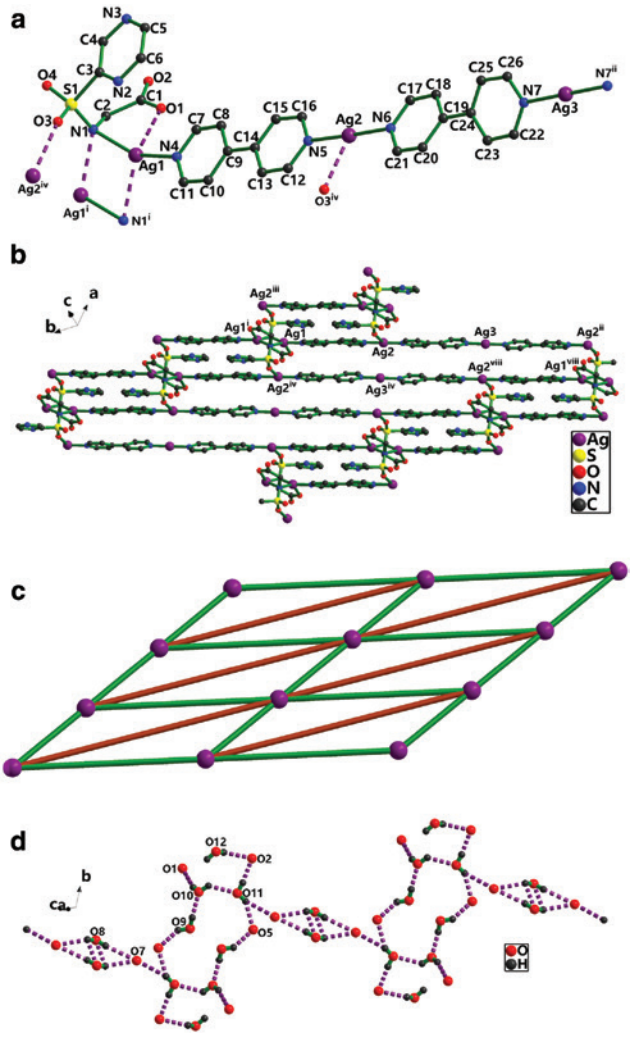

Fig. 2: (a) The coordination environment for Ag^+ in **2** (symmetry codes: i: $-x+1$, $-y$, $-z+1$; ii: $-x+2$, $-y+4$, $-z+2$; iv: $-x+1$, $-y+1$, $-z+1$). (b) The Ag-pby chain in **2** (symmetry codes: i: $-x+1$, $-y$, $-z+1$; ii: $-x+2$, $-y+4$, $-z+2$; iv: $-x+1$, $-y+1$, $-z+1$; viii: x, $y-1$, z). (c) The simplified representation of the 2D (3, 6) grid network (green lines represent bpy ligand, brown lines represent $Ag(bpy)_2$) chains. (d) View of O–H···O hydrogen bonded rings in **2**.

silver ions to the pyridyl sites is manifested by the relatively short Ag–N bond distances. In **2**, these are Ag1–N 2.224(4) and 2.281(4) Å, Ag2–N 2.164(4) and 2.170(4) Å, and Ag3–N 2.147(4) Å, with additional binding of Ag1 and Ag2 to the carboxylate, sulfonyl, and imine function of the bridging ligand L^{2-} (Fig. 1a). The inversion-related Ag1 pair is coordinated from both sides in a μ_2-η^1:η^1 bridging mode by carboxylate and imine groups at relatively long Ag–O and Ag–N distances of 2.566(5) and 2.626(4) Å, with an Ag···Ag separation of 2.8777(9) Å, implying the existence of ligand-supported argentophilic interactions. Ag2 is coordinated in a monodentate fashion to one of the sulfonyl O atoms at Ag2–O = 2.66(8) Å, forming $[Ag_4L_2]$ secondary building units (SBUs between adjacent [Ag-bpy] polymeric chains). Ag3 lies at an inversion center, coordinated by two symmetry-related bpy in a μ_2-η^1:η^1 bridging mode. Taking weak Ag–O/N interactions into account, the coordination mode of L^{2-} can be denoted as μ_3-(η_2-O,N),N,O′ in **2**. There are open voids within the 2D array (Fig. 2b), as there is an alternating connection with bpy between the Ag1, Ag2, and Ag3 metal nodes of neighboring chains in the layer. These voids contain solvent molecules and NO_3^- anions. From the topological point of view, each $[Ag_4L_2]$ SBU links four bpy and two $Ag(bpy)_2$ as a six-connected node, and each bpy or $Ag(bpy)_2$ bridges two $[Ag_4L_2]$ acting as a linker. The 2D MOF structure of **2** can be simplified as a six-connected (3, 6) grid layer topology (Fig. 1c). On the other hand, each $[(Ag_4L_2)(bpy)]_2$ unit serves as a four-connected node, and each $[Ag(bpy)_2]^+$ acts as a linker. The 2D MOF structure of **2** can be simplified as a four-connected (4, 4) grid layer topology.

The stacking between the 2D polymeric arrays in structure **2** is further stabilized by numerous hydrogen bonding interactions, involving the water molecules, the NO_3^- anions, and the carboxylate groups. Intermolecular O–H···O hydrogen bonds constitute R_8^{16}, R_4^8, R_3^4, and R_2^4 rings [27] with the solvate H_2O (O8, donor and acceptor; O9, O10, O11, and O12, donors), the nitrate O atoms

(O5 and O7, acceptors), and the carboxylate moiety (O1 and O2, acceptors). O12···O1 and H12A···O1 distances of 4.39(8) and 3.84(3) Å, respectively, are too long to form an effective hydrogen bond, resulting in an open-loop R_4^{10}. These rings alternate by translation along the *c* axis (Fig. 2d and Table 2) and link the grid layers in reversely alternating parallel arrangements, defining a 3D hydrogen-bonded network supporting the supramolecular architecture. Furthermore, between adjacent layers, there exists a pair of π stacking interactions between the pyridine rings (N4–C7–C8–C9–C10–C11, N5–C12–C13–C14–C15–C16, N6–C17–C18–C19–C20–C21, and N7–C22–C23–C24–C25–C26) (face-to-face). The dihedral angles between the two planes are 4.5(3) and 26.6(3)°, respectively, with centroid-to-centroid distances of 3.826(3) and 3.937(3) Å. Thus, these layers are extended into an interwoven 3D supramolecular architecture through O–H···O and π···π interactions.

2.3 Infrared spectra of 1 and 2

Complexes **1** and **2** exhibit infrared bands in the range 4000–450 cm^{-1}, which are different from those of the free ligand. The band ν(NH) = 3278 cm^{-1} of the H_2L molecule is absent in the spectra of **1** and **2** indicating the deprotonation of the imine N atom upon coordination to the metal ion. Bands assigned to $\nu_{as}(COO^-)$ and $\nu_s(COO^-)$, which are observed for the free ligand at 1730 and 1406 cm^{-1}, respectively, are shifted to 1586 for **1**, 1598 for **2** and 1398 for **1**, 1404 cm^{-1} for **2**, indicating that deprotonation of the carboxylate groups occurred upon coordination. The $\nu_{as}(-SO_2-)$ (1330 cm^{-1} for H_2L, 1223 cm^{-1} for **1**, and 1218 cm^{-1} for **2**) and $\nu_s(-SO_2-)$ (1128 cm^{-1} for H_2L, 1045 cm^{-1} for **1**, and 1086 cm^{-1} for **2**) bands show differences from that of H_2L, suggesting that this group does also interact with the metal ion. Bands centered at 3406, 1384, and 853 cm^{-1} ascribed to H_2O and $\nu_{as}(NO_3^-)$, $\nu_s(NO_3^-)$ for **2**, are absent in the spectra of **1**. All these spectroscopic features of H_2L and **1**, **2** are consistent with the crystal structure determinations.

3 Conclusions

In summary, two Ag-MOFs based on the L^{2-} ligand with different structural motifs have been synthesized and characterized. They show distinct topologies of 3D supramolecular structures in the solid state supported by the combination of coordinative bonds, ligand-supported Ag···Ag interactions, and weak Ag···O/N coordinative interactions or intermolecular hydrogen bonding and aromatic π–π interactions.

4 Experimental

4.1 Materials and physical methods

H_2L was synthesized by the literature methods [28, 29]. All other chemicals were commercially available and used as received without further purification. The elemental analyses (C, H, N, and S) were performed on a Perkin-Elmer 240C apparatus. FT-IR spectra were recorded from KBr pellets in the range of 4000–450 cm^{-1} on a Varian FT-IR 640 spectrometer.

4.2 Synthesis of $[Ag_2(L)]_n$ (1)

H_2L (0.043 g, 0.2 mmol) dissolved in distilled water (5 mL) was added dropwise to a stirred solution of excessive $AgNO_3$ (0.085 g, 0.5 mmol) in ethanol (10 mL). The pH value was adjusted to about 7.0 with 0.1 mol L^{-1} NaOH solution, and the resulting mixture was stirred at 333 K for 2 h, cooled to room temperature, and filtered. The filtrate was allowed to slowly concentrate by evaporation at room temperature. Two weeks later, colorless block-shaped crystals suitable for X-ray structure analysis were obtained in a yield of 30% (based on Ag). – $C_6H_5Ag_2N_3O_4S$ (430.93): calcd. C 16.71, H 1.16, N 9.75, S 7.43; found C 17.69, H 1.18, N 9.76, S 7.45. – IR (KBr): ν = 1586 (s), 1456 (w), 1398 (s), 1336 (w), 1305 (m), 1223 (m), 1178 (m), 1090 (m), 1045 (w), 1017 (w), 921 (m), 605 (m) cm^{-1}.

4.3 Synthesis of $\{[Ag_{2.5}(L)(4,4'\text{-bipy})_2]\cdot(NO_3)_{0.5}\cdot(H_2O)_{4.5}\}_n$ (2)

H_2L (0.043 g, 0.2 mmol) dissolved in distilled water (5 mL) was added dropwise to a stirred solution of $AgNO_3$ (0.085 g, 0.5 mmol) in ethanol (10 mL). The pH value was adjusted to about 7.0 with 0.1 mol L^{-1} NaOH solution, and the resulting mixture was stirred at 333 K for 2 h. Then 2 mL of an ethanol solution of 4,4′-bipyridine (0.064 g, 0.4 mmol) was added slowly, and the stirring continued for 2 h. The mixture was cooled to room temperature, and filtered. The filtrate was allowed to slowly concentrate by evaporation at room temperature. Two weeks later, colorless block-shaped crystals suitable for X-ray structure analysis were obtained in a yield of 25% (based on Ag). – $C_{26}H_{30}Ag_{2.5}N_{7.5}O_{10}S$ (909.31):

calcd. C 34.31, H 3.30, N 11.55, S 3.52; found C 34.32, H 3.28, N 11.57, S 3.50. – IR (KBr): ν = 3406 (m), 1598 (s), 1530 (w), 1484 (w), 1404 (s), 1384 (s), 1218 (m), 1174 (m), 1086 (m), 1042 (w), 853 (m), 620 (m) cm^{-1}.

4.4 Crystal structure determinations

Single-crystal data collections were performed on a Bruker Smart Apex II CCD diffractometer with graphite-monochromatized MoK_α radiation (λ = 0.71073 Å) at 296(2) K. The structures were solved with Direct Methods using SHELXS-97 [30, 31], and structure refinements were performed against F^2 using SHELXL-97 [32, 33]. All non-hydrogen atoms were refined with anisotropic displacement parameters. Carbon-bound H atoms were placed in calculated positions ($d_{C–H}$ = 0.93–0.97 Å) and were included in the refinement in the riding model approximation, with U_{iso}(H) set to 1.2U_{eq}(C). The H atoms of coordinating water in **2** were located in difference Fourier maps, and were refined with distance restraints of $d_{O–H}$ = 0.85 ± 0.01 Å and H···H 1.387 ± 0.02 Å. Their displacement parameters were tied to those of the parent atoms by a factor of 1.5. The maximum residual electron density peaks of 1.61 e Å^{-3} for **1** and 1.29 e Å^{-3} for **2** were located 1.31 Å from the Ag1 atom for **1** and 0.60 Å from the N8 atom for **2**. DFIX, SADI, and DANG instructions from SHELXL have been applied to constrain some O–H, N–O and H···H distances in **2**. Further details of the structure determinations are summarized in Table 3.

CCDC 1481728 (**1**) and CCDC 1481729 (**2**) contain the supplementary crystallographic data for this paper. These data can be obtained free of charge from The Cambridge Crystallographic Data Centre via http://www.ccdc.cam.ac.uk/data_request/cif.

Table 3: Crystal structure data for **1** and **2**.

Compound	**1**	**2**
Formula	$C_6H_5Ag_2N_3O_4S$	$C_{26}H_{30}Ag_{2.5}N_{7.5}O_{10}S$
M_r	430.93	1818.62
Crystal size, mm^3	0.40 × 0.20 × 0.12	0.30 × 0.20 × 0.12
Crystal system	Monoclinic	Triclinic
Space group	$P2_1/n$	$P\bar{1}$
a, Å	5.9211(5)	10.3159(6)
b, Å	17.2762(14)	12.7795(6)
c, Å	9.3789(9)	13.4463(7)
α, deg	90	98.729(4)
β, deg	98.457(9)	97.994(4)
γ, deg	90	108.171(5)
V, Å^3	948.97(14)	945.39(9)
Z	4	2
$D_{calcd.}$, g cm^{-3}	3.02	1.85
μ(MoK_α), mm^{-1}	4.3	1.6
F(000), e	816	452
hkl range	−6 → 7, ±20, ±11	±12, −15→14, −16→15
$((\sin\theta)/\lambda)_{max}$, Å^{-1}	0.597	0.625
Refl. measured	7142	11 999
Refl. unique/R_{int}	1676/0.0599	6662/0.022
Param. refined	145	467
$R1^a$/$wR2^b$ [$I>2\sigma(I)$]	0.0441/0.1005	0.0523/0.1418
$R1^a$/$wR2^b$ (all data)	0.0489/0.1043	0.0636/0.1498
GoF (F^2)^c	1.07	1.098
$\Delta\rho_{fin}$ (max/min), e Å^{-3}	1.61/−0.94	1.29/−0.85

$^a R1 = \Sigma||F_o| - |F_c||/\Sigma|F_o|$.

$^b wR2 = [\Sigma w(F_o^2 - F_c^2)^2/\Sigma w(F_o^2)^2]^{1/2}$, $w = [\sigma^2(F_o^2) + (AP)^2 + BP]^{-1}$, where $P = (\mathrm{Max}(F_o^2, 0) + 2F_c^2)/3$.

$^c \mathrm{GoF} = S = [\Sigma w(F_o^2 - F_c^2)^2/(n_{obs} - n_{param})]^{1/2}$.

Acknowledgments: This work was supported by the Guangxi Provincial Department of Education (Nos. KY2015ZD130, YB2014414) and the Natural Science Foundation of Guangxi Province (Nos. 2014GXNSFAA118035, 2014GXNSFBA118040). The support of the National Natural Science Foundation of China (No. 51402158) is gratefully acknowledged. The authors also acknowledge the financial support by the Opening Project of Guangxi Colleges and Universities Key Laboratory of Beibu Gulf Oil and Natural Gas Resource Effective Utilization (Nos. 2015KLOG09, 2014PY-GJ05).

References

[1] M. P. Komal, E. D. Michelle, T. Thomas, C. M. Stephen, R. H. Lyall, *Cryst. Growth Des*. **2016**, *16*, 1038.
[2] Y. Zhao, N. Kornienko, Z. Liu, C. Zhu, S. Asahina, T. R. Kuo, W. Bao, C. Xie, A. Hexemer, O. Terasaki, P. Yang, O. M. Yaghi, *J. Am. Chem. Soc*. **2015**, *137*, 2199.
[3] G. Zhan, H. C. Zeng, *Adv. Funct. Mater*. **2016**, *26*, 3268.
[4] S. Choi, H. J. Lee, M. Oh, *Small* **2016**, *12*, 2425.
[5] Z. Wang, X. Y. Li, L. W. Liu, S. Q. Yu, Z. Y. Feng, C. H. Tung, D. Sun, *Chem. Eur. J*. **2016**, *22*, 6830.
[6] Y. Zhang, L. Huang, H. Miao, H. X. Wan, H. Mei, Y. Liu, Y. Xu, *Chem. Eur. J*. **2015**, *21*, 3234.
[7] K. Shiva, K. Jayaramulu, H. B. Rajendra, M. Kumar, B. Tapas, J. Aninda, *Z. Anorg. Allg. Chem*. **2014**, *640*, 1115.
[8] Q. L. Zhu, Q. Xu, *Chem. Soc. Rev*. **2014**, *43*, 5468.
[9] J. Wang, Y. Wei, G. Jason, G. Yi, Y. Zhang, *Chem. Commun*. **2015**, *51*, 15708.
[10] S. Xiong, Q. Liu, Q. Wang, W. Li, Y. Tang, X. Wang, S. Hu, B. Chen, *J. Mater. Chem. A* **2015**, *3*, 10747.
[11] Z. Zeng, Y. Zhong, H. Yang, R. Fei, R. Zhou, R. Luque, Y. Hu, *Green Chem*. **2016**, *18*, 186.
[12] H. Yang, R. L. Sang, X. Xu, L. Xu, *Chem. Commun*. **2013**, *49*, 2909.
[13] Y. L. Wang, Q. Y. Liu, X. Li, *CrystEngComm* **2008**, *10*, 1667.
[14] H. M. Titi, I. Goldberg, *CrystEngComm* **2010**, *12*, 3914.

[15] A. Karmakar, I. Goldberg, *CrystEngComm* **2011**, *13*, 350.
[16] G. P. Yang, J. H. Zhou, Y. Y. Wang, P. Liu, C. C. Shi, A. Y. Fu, Q. Z. Shi, Q. Y. Liu, X. Li, *CrystEngComm* **2011**, *13*, 33.
[17] S. M. Fang, M. Hu, Q. Zhang, M. Du, C. S. Liu, *Dalton Trans.* **2011**, *40*, 4527.
[18] B. Li, S. Q. Zang, C. Ji, C. X. Du, H. W. Hou, T. C. W. Ma, *Dalton Trans.* **2011**, *40*, 788.
[19] Y. L. Wei, X. Y. Li, T. T. Kang, S. N. Wang, S. Q. Zang, *CrystEngComm* **2014**, *16*, 223.
[20] H. Schmidbaur, A. Schier, *Angew. Chem., Int. Ed.* **2015**, *54*, 746.
[21] F. Zhao, H. Dong, B. Liu, G. Zhang, H. Huang, H. Hu, Y. Liu, Z. Kang, *CrystEngComm* **2014**, *16*, 4422.
[22] A. Karmakar, H. M. Titi, I. Goldberg, *Cryst. Growth Des*. **2011**, *11*, 2621.
[23] G. P. Yang, Y. Y. Wang, P. Liu, A. Y. Fu, Y. N. Zhang, J. C. Jin, Q. Z. Shi, *Cryst. Growth Des*. **2010**, *10*, 1443.
[24] B. Li, S. Q. Zang, C. Ji, H. W. Hou, T. C. W. Mak, *Cryst. Growth Des*. **2012**, *12*, 1443.
[25] P. X. Yin, J. Zhang, Z. J. Li, Y. Y. Qin, J. K. Cheng, L. Zhang, Q. P. Lin, Y. G. Yao, *Cryst. Growth Des*. **2009**, *9*, 4884.
[26] L. Yang, D. R. Powell, R. P. Houser, *Dalton Trans.* **2007**, *36*, 955.
[27] J. Bernstein, R. E. Davis, L. Shimoni, N. L. Chang, *Angew. Chem., Int. Ed. Engl*. **1995**, *34*, 1555.
[28] S. W. Wright, K. N. Hallstrom, *J. Org. Chem*. **2006**, *71*, 1080.
[29] L. F. Ma, L. Y. Wang, J. G. Wang, Y. F. Wang, X. Feng, *Inorg. Chim. Acta* **2006**, *7*, 2241.
[30] G. M. Sheldrick, SHELXS-97, Program for the Solution of Crystal Structures, University of Göttingen, Göttingen (Germany) **1997**.
[31] G. M. Sheldrick, *Acta Crystallogr*. **1990**, *A46*, 467.
[32] G. M. Sheldrick, SHELXL-97, Program for the Refinement of Crystal Structures, University of Göttingen, Göttingen (Germany) **1997**.
[33] G. M. Sheldrick, *Acta Crystallogr*. **2008**, *A64*, 112.